

ANALYSIS OF THE EFFECT OF TOOL GEOMETRY ON THE SHEAR ANGLE IN METAL CUTTING

Д. ВАРГА

АНАЛІЗ ВПЛИВУ ГЕОМЕТРИЧНИХ ПАРАМЕТРІВ ІНСТРУМЕНТУ НА КУТ ЗСУВУ ПРИ ОБРОБЦІ

Аналіз, що базується на методі скінчених елементів, дозволив моделювати процес різання, і має деякі переваги для прогнозування розподілу зусиль і температур, оцінки зношування інструмента й залишкових напруг в обробленій деталі, також допомагає оптимізувати геометрію різального інструменту й режими різання. Однак, напруга пластичного плинину матеріалу оброблюваної деталі й характеристики тертя в зоні різання не завжди можливо спрогнозувати. У цій роботі використовується проста модель різання, показані результати. Модель тертя заснована на оцінці нормального розподілу напруги по передній поверхні. Зміна кута зсуву й різальних сил для різних матеріалів заготовок в процесі відбиті в даній роботі.

Анализ, базирующийся на методе конечных элементов, позволил моделировать процесс резания, и имеет некоторые преимущества для прогнозирования распределения усилий и температур, оценки износа инструмента и остаточных напряжений в обработанной детали, также помогает оптимизировать геометрию режущего инструмента и режимы резания. Однако, напряжение пластического течения материала обрабатываемой детали и характеристики трения в зоне резания не всегда возможно спрогнозировать. В этой работе используется простая модель резания, показаны результаты. Модель трения основана на оценке нормального распределения напряжения по передней поверхности. Изменение угла сдвига и режущих сил для различных материалов заготовки в процессе отражены в данной работе.

Finite element analysis based techniques are available to simulate cutting processes and offer several advantages including prediction of tool forces, distribution of stresses and temperatures, estimation of tool wear and residual stresses on machined surfaces, optimization of cutting tool geometry and cutting conditions. However, workpiece material flow stress and friction characteristics at cutting zones are not always available. This paper utilizes a simple metal cutting model and shows running results. The friction model is based on estimation of the normal stress distribution over the rake face. The changing of shear angle and cutting forces in cutting of different workpiece material in the beginning of cutting is shown in this paper.

INTRODUCTION

The Finite Element examinations are applied for the simulation of metal cutting processes. More than a century ago the modelling of chip formation was based on the shear model [1] or the slip-line theory [2]. At that time these models were very effective, but later they could not support of studying the non-linear behaviour of workpiece material. Nowadays, the Finite Element Method has particularly become the main tool for simulation of the metal cutting process, and there is software that provides simulation function of the orthogonal cutting [3], [4]. The finite element method provides possibility for solving non-linear problems. Simulations of FEM are very time consuming and the accuracy of results always need to be improved.

For simulation of cutting process, both the Lagrangian approach and the Eulerian approach [5] have been used extensively. These models provide information about stresses and strain fields, shear zones, and temperature field when the model includes thermo-mechanical coupling [6], [19].

As the real cutting process is very sophisticated and influenced by many parameters, it is very difficult to create an almost real model for the primary shear zone. The engineering approach to the description the character of plastic deformation in the shear zone is based on some simplifications. The most commonly used models for the primary shear zone are [7]:

- Merchant's single-shear plane model;
- Oxley's parallel-sided shear-zone model;
- Zorev's pie-shaped shear-zone model [8], as shown in Fig. 1 [9].

According to Astakhov et al. [10] the shear zone can be divided into two regions:

- wide region where the velocity change takes places at a low rate, and
- narrow region where this change takes place at a high rate.

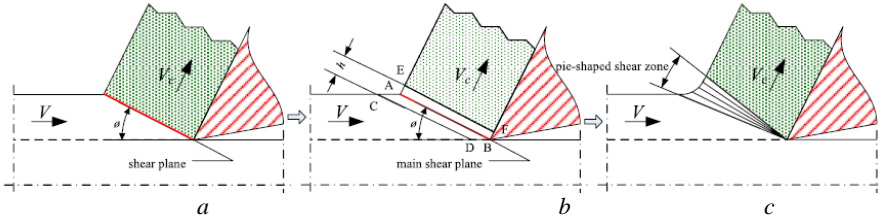


Figure 1 – Shear zone models: a – single-shear plane model, b – parallel-sided shear plain model, c – pie-shaped shear plain model

In this paper, the aim is to concentrate the initial steps of cutting. The aim is to analyse how the tool geometry effects on the angle of the shear plane.

1. BACKGROUNDS OF FINITE ELEMENT EXAMINATIONS

For dynamic equilibrium of a body, the equation (1) at time t_n irrespective of material behaviour can be constructed based on the Principle of Virtual Work [11] :

$$\int_{\Omega} [\delta \epsilon_n]^T \sigma_n d\Omega - \int_{\Omega} [\delta u_n]^T [b_n - \rho_n \ddot{u}_n - \dot{c}_n \dot{u}_n] d\Omega - \int_{\Gamma_t} [\delta u_n]^T t_n d\Gamma = 0 \quad (1)$$

Where $\delta \mathbf{u}_n$ is the vector of virtual displacements, $\delta \boldsymbol{\varepsilon}_n$ is the associated virtual strains, \mathbf{b}_n is the vector of applied body forces, \mathbf{t}_n is the vector of surface tractions, $\boldsymbol{\sigma}_n$ is the vector of stresses, ρ_n is the mass density, \mathbf{c}_n is the damping parameter and refers to differentiation with respect to time. Ω_n is the domain of interest, has two boundaries: Γ_t boundary on which boundary conditions \mathbf{t}_n are specified and Γ_u boundary on which displacements \mathbf{u}_n are specified.

For a finite-element representation, the displacements and strains and their virtual counterparts are given by the expressions as [15]

$$\mathbf{u}_n = \sum_{i=1}^m \mathbf{N}_i [\mathbf{d}_i]_n, \quad \delta \mathbf{u}_n = \sum_{i=1}^m \mathbf{N}_i [\delta \mathbf{d}_i]_n \quad (2)$$

$$\boldsymbol{\varepsilon}_n = \sum_{i=1}^m \mathbf{B}_i [\mathbf{d}_i]_n, \quad \delta \boldsymbol{\varepsilon}_n = \sum_{i=1}^m \mathbf{B}_i [\delta \mathbf{d}_i]_n \quad (3)$$

where at the time t_n for node i vector of nodal displacement is $[\mathbf{d}_i]_n$, and the vector of virtual nodal variables is $[\delta \mathbf{d}_i]_n$, \mathbf{N}_i is the global shape functions matrix and \mathbf{B}_i is the global stain-displacement matrix. The total number of nodes is m . After substituting these equations into Eqn. (1), the resulting equation is true for any set of virtual displacements, then we can obtain for each node i the equations [11] as,

$$[\mathbf{p}_i]_n - [\mathbf{f}_{Bi}]_n + [\mathbf{f}_{fi}]_n + [\mathbf{f}_{Di}]_n - [\mathbf{f}_{Ti}]_n = 0 \quad (4)$$

where the internal resisting forces are

$$[\mathbf{p}_i]_n = \int_{\Omega} [\mathbf{B}_i]^T \boldsymbol{\sigma}_n d\Omega \quad (5)$$

the consistent forces for the applied body forces are

$$[\mathbf{f}_{Bi}]_n = \int_{\Omega} [\mathbf{N}_i]^T \mathbf{b}_n d\Omega \quad (6)$$

the inertial forces are

$$[\mathbf{f}_{fi}]_n = \int_{\Omega} [\mathbf{N}_i]^T \rho_n [\mathbf{N}_1, \mathbf{N}_2, \dots, \mathbf{N}_m] d\Omega \begin{bmatrix} [\ddot{\mathbf{d}}_1]_n \\ [\ddot{\mathbf{d}}_2]_n \\ \vdots \\ \vdots \\ [\ddot{\mathbf{d}}_m]_n \end{bmatrix} \quad (7)$$

the damping forces are

$$[\mathbf{f}_{Di}]_n = \int_{\Omega} [\mathbf{N}_i]^T \mathbf{c}_n [\mathbf{N}_1, \mathbf{N}_2, \dots, \mathbf{N}_m] d\Omega \begin{bmatrix} [\dot{\mathbf{d}}_1]_n \\ [\dot{\mathbf{d}}_2]_n \\ \vdots \\ [\dot{\mathbf{d}}_m]_n \end{bmatrix} = \sum_{j=1}^m [\mathbf{C}_{ij}]_n [\dot{\mathbf{d}}_j]_n \quad (8)$$

and the consistent forces for the boundary forces are

$$[\mathbf{f}_{Ti}]_n = \int_{\Gamma_i} [\mathbf{N}_i]^T \mathbf{t}_n d\Omega \quad (9)$$

The displacements can be expressed in the usual form [11] as

$$[\mathbf{u}^{(e)}]_n = \sum_{i=1}^r \mathbf{N}_i^{(e)} [\mathbf{d}_i^{(e)}]_n \quad (10)$$

where r is 8 for 8-noded isoparametric elements. Similarly, for the each element the strain displacement relationships can also be written.

2. JOHNSON-COOK FORMULATION

2.1. Constitutive equation

Flow stress models are considered to represent work material constitutive behaviour under machining conditions. A lot of empirical and semi-empirical constitutive models have been developed to model flow stress with certain accuracy in machining [12]. Most of these constitutive models are based on different assumptions to avoid the prevailing complexities of stress state exist in machining. The strain rate and temperature coupling effect is especially important at high cutting speeds where thermal softening becomes more dominant due to increased heat generation. A detailed discussion about work material considerations is given in Asstakhov [13]. Numeric simulation of chip formation requires a thermo-visco-plastic law. Among other material constitutive models, model by Johnson and Cook [14] is widely used for high-strain rate applications. This constitutive model describes the flow stress of a material with the product of strain, strain rate and temperature effects that are individually determined as given in Eq. 3.1.

$$\sigma_{eq} = (A + B\varepsilon^n) \left[1 + C \ln \left(\frac{\dot{\varepsilon}}{\dot{\varepsilon}_0} \right) \right] \left[1 - \left(\frac{T - T_{room}}{T_{melt} - T_{room}} \right)^m \right] \quad (11)$$

Where σ_{eq} the flow stress, ε effective plastic strain, $\dot{\varepsilon}$ effective plastic strain rate, T temperature, $\dot{\varepsilon}_0$ reference plastic strain rate, T_{room} room temperature, T_{melt} melting temperature, A , B , C , n , m rheological parameters.

The first part of Eq. (11) defines the strain rate hardening, the middle part of the strain rate sensitivity and the last one of the thermal softening of the material.

The constants of the Johnson-Cook material for A45 steel and EN GJL 200 cast iron are given in Table 1. [15]

Table 1 – Constants of Johnson-Cook material model [15]

Material	A, MPa	B, MPa	n	C	m	$T_{melt}, ^\circ C$
AISI 1045	553.1	600.8	0.234	0.013	1.00	1460

2.2 Friction at the tool-chip interface

Astakhov summarised a lot of studies in his book [13] about stress distributions at the tool-chip interface. Zorev proposed [8] and utilised others e.g. Dirikolu et al., [16] and Özel and Altan, [17] how the normal σ_n and shear stress distributions can be assumed on the tool rake face. According to Zorev’s model, a sticking region forms in the tool-chip contact area near the cutting edge. The assumed formula for frictional shear stress distribution (τ_f) on the tool rake face can be represented in two distinct regions, at the sticking region by (Eq. 12) and at the sliding region by (Eq. 13) [8]:

$$\tau_f(y) = k_{chip} \quad \text{and when} \quad \mu\sigma_n(y) \geq k_{chip} \quad A < y \leq B \quad (12)$$

$$\tau_f(y) = \mu\sigma_n(y) \quad \text{and when} \quad \mu\sigma_n(y) < k_{chip} \quad B < y \leq C \quad (13)$$

where:

k_{chip} average shear flow stress at tool-chip interface,

y co-ordinate on main cutting edge of cutting tool (Fig. 2),

A, B, C points along the main cutting edge (Fig. 2).

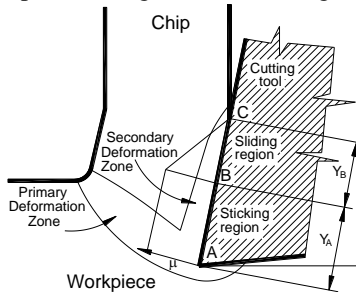


Figure 2 – Deformation zones and the distortion of friction coefficient along the contact line on the cutting tool chip interface

3. THE USE OF FINITE ELEMENT METHOD FOR SIMULATION OF ORTHOGONAL METAL CUTTING PROCESS

The modelling of cutting process requires sub tasks, as modelling of cutting tool, chip formation modelling - element separation, adaptive meshing, and determination of parameters of the analysis. The most important parameters of finite

element simulation of metal cutting can be demonstrated in Fig. 3 [18]. In this paper we examined material qualities: steel AISI 1045 and cast iron EN-GJL-200. Calculated depth of cut $a = 1.0\text{mm}$ and feed rate $f = 0.5\text{mm/rev}$. From the calculated parameters we only show the results of Mises stress ones in Fig. 3 after the machined length ($x=0,3\text{mm}$ and $x=3\text{mm}$).

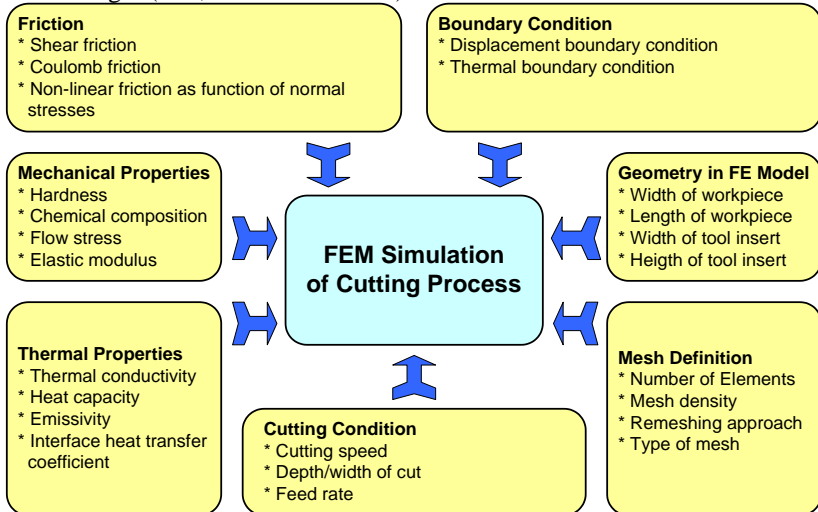


Figure 3 – Input parameters for simulation of cutting process [18]

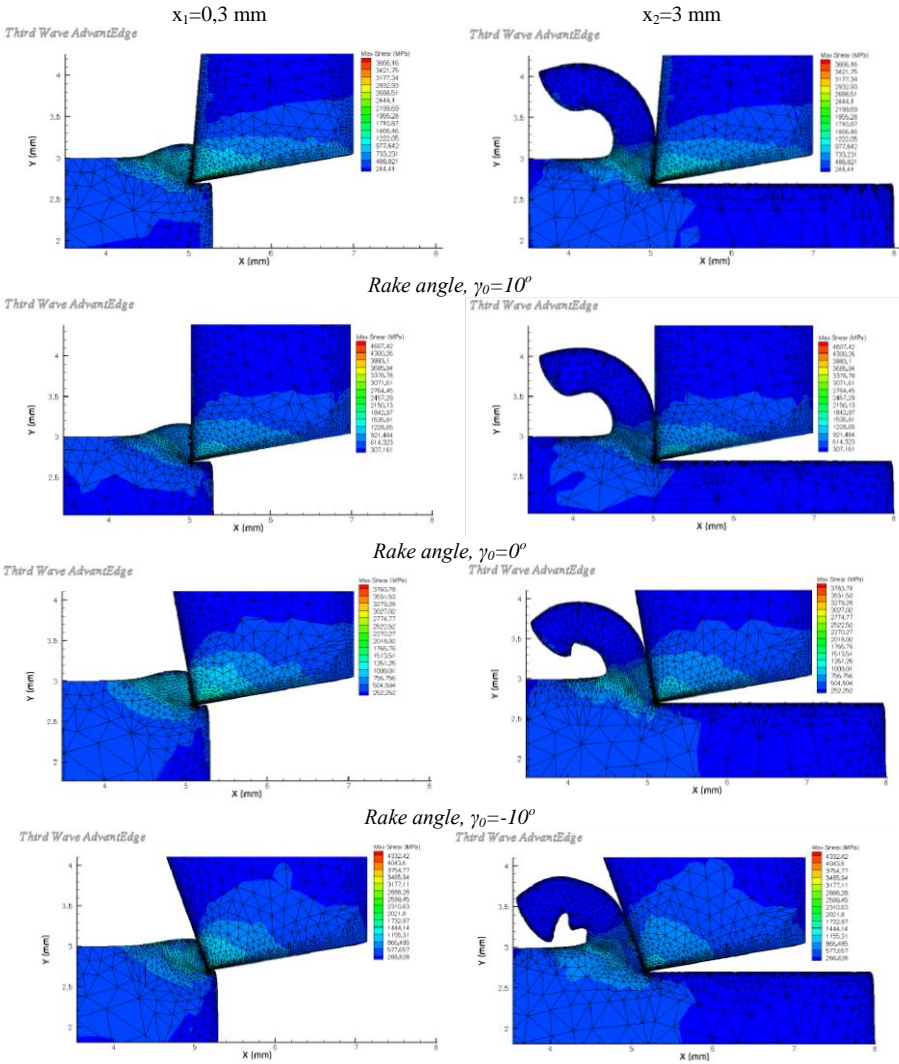
Earlier models of metal cutting were based on only basic shear plane assumption or slip line field analysis[20]. Iwata [21] incorporated the frictional stress as a function of normal stress at the boundary conditions with an empirical relationship based on a coefficient of friction obtained from friction tests. Capabilities in generating a very dense mesh near the tool tip and remeshing adaptively makes this software applicable to simulate the cutting process. In order to cope with the geometrical and material non-linearity and the contact conditions between the cutting tool and boundary nodes of the workpiece, the finite element simulation is conducted incrementally [22]

3.1 Cutting tool modelling

The cutting tool is assumed as rigid and subjected to translation movement only, i.e. the effects of the tool deformation and the vibration of the machine tool are not considered in this study. Displacement increments are applied as the cutting tool moves ahead, and the element stresses and the cutting forces are obtained as a result of the contact deformations between the deformable workpiece and the rigid cutting tool.

3.2 Chip formation modelling - element separation

Great efforts have been made for understanding the mechanisms of chip formation and the role of effective parameters. The continuous separation of the workpiece to form a chip can be modelled using the finite element method as a sequence of separations between elements along a prescribed line in front of the tool tip and parallel to the cutting direction [23].



Rake angle, $\gamma_0=-10^\circ$

Figure 4 – Illustration of chip formation and creation of Max Shear Stress for cutting tools having different rake angles.

3.3 Adaptive meshing.

At cutting large plastic strains occurs due to high deformations in the elements. Severe distortion in the elements can be controlled by adaptive meshing. Adaptive meshing can be done by using moving nodes, splitting elements or re-

meshing the model. This can be used to reduce element distortion or refine meshing areas where error estimates are highest [24]. During the metal cutting process, the finite element mesh is adaptively modified when the coarse mesh ahead of the cutting tool is close to the primary deformation zone. Four types of mesh rezoning techniques are used. The elemental and nodal data, such as stresses, strains, temperatures, etc., are interpolated, deleted, added or translated during the mesh rezoning [25].

3.4 Parameters of the analysis

In the examined case: material quality: A45
 depth of cut: a = 0.1 mm.
 feedrate: f = 0.3 mm/rev.

Coating of carbide cutting tool was TiAlN. Fig. 4 illustrates the shear angles using the result of maximum values of shear stresses. On the left hand side column shows the situation almost in the beginning ($x=0.3\text{mm}$) of the metal cutting, while on the right hand side column demonstrates the situations of metal cutting after machining 3mm by the cutting tool. In the first row the value of the rake angle is 10 degrees, while in the second row is zero, in the third row is minus 10, and in the fourth row is minus twenty. Fig. 5 demonstrates the values of shear angles for four different rake angles. Although the Shear Plane Angles vary in the function of the machined length, results show good agreement with theory. As the value of rake angle is reducing, the shear plane angle is reducing too.

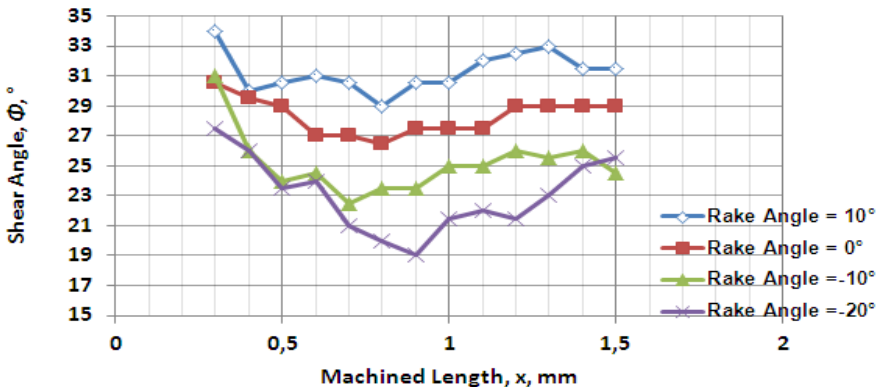


Figure 5 – Shear angles in the function of machined length of Steel AISI-1045

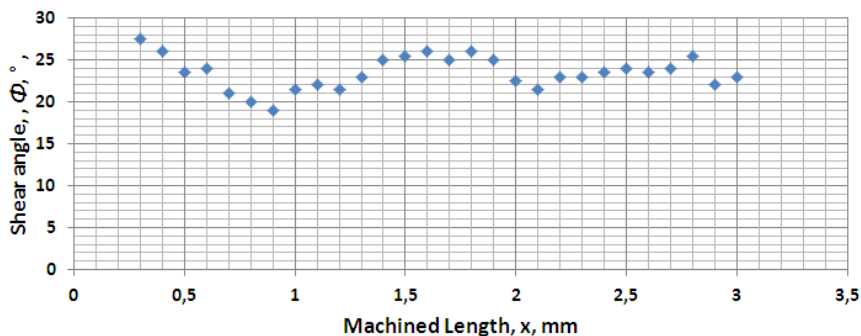


Figure 6 – Shear angles in the function of machined length of Steel AISI-1045 with the rake angle minus 20 degree.

Figure 6 Shows only that case when the rake angle is minus 20 degrees. As the chip formation is fluctuating, the shear plane angle is fluctuating as well.

CONCLUSIONS

This paper contains a brief summary about the development of Finite Element Simulation of metal cutting and shows our results. The simulation results show the shear angles occurring in case of Steel AISI-1045 material. At the beginning of cutting, shear angle is decreasing at work material steel AISI-1045. Stress distributions and temperature on tool-chip interface were studied, which parameters are very difficult to measure by experiment. In addition to this the FE model can be used to choose optimal cutting parameters. It can be used to design for cutting tool profile as well, so in this way the very expensive experiments can be avoided.

ACKNOWLEDGEMENT

“The described work was carried out as part of the TÁMOP-4.2.1.B-10/2/KONV-2010-0001 project in the framework of the New Hungarian Development Plan. The realization of this project is supported by the European Union, co-financed by the European Social Fund.”

References 1 Merchant, E.: **Basic mechanics of metal-cutting processes**, Journal of Applied Mechanics, Vol.: 66, 1944, p. 168-175. 2 Lee, E., Shaffer, B.: **The theory of plasticity applied to a problem of machining**, Journal of Applied Mechanics, Vol.: 73, 1951, p. 404-413. 3 Third Wave AdvantEdgeTM (2006) Third Wave system Inc., Minneapolis, USA. 4 Mamalis AG, Kundrak J, Markopoulos A, Manolakos DE: **On the finite element modelling of high speed hard turning**, International Journal of Adv. Manuf. Technol (2008) 38: (5-6) pp. 441-446. 5 Movahhedy M., Gadala M.S., Altintas Y.: **Simulation of the orthogonal metal cutting process using an arbitrary Lagrangian-Eulerian Finite-element**

method, Journal of Materials Processing Technology 103 (2000) 267-275, **6** Pantalé O., Bacaria J.-L., Dalverny O., Rakotomalala R., Caperaa S.: **2D and 3D numerical models of metal cutting with damage effects**, Computational Methods Appl. Mech. Engineering 193 (2004) 4383-4399, **7** Grzesik W (2008) **Advanced machining processes of metallic materials**. Elsevier, London **8** Zorev, N. N.: **Metal Cutting Mechanics**, Oxford, UK: Pergamon Press. 1966 **9** Binglin Li, Xuelin Wang, Yujin Hu, Chenggang Li: **Analytical prediction of cutting forces in orthogonal cutting using unequal division shear-zone model**, Int J Adv Manuf Technol (2011) 54:431-443 **10** Astakhov VP, Osman MOM, Hayajneh MT (2001) Re-evaluation of the basic mechanics of orthogonal metal cutting: velocity diagram, virtual work equation, and upper bound theorem. Int J Mach Tools Manuf 41:393-418 **11** Ramesh MV., Chan KC, Lee WB, Cheung CF: **Finite-element analysis of diamond turning of aluminium matrix composites**, Composites Science and Technology 61 (2001) pp.: 1449-1456 **12** Özel, T., Zeren, E. **Numerical modelling of meso-scale finish machining with finite edge radius tools**, International Journal of Machining and Machinability of Materials, Vol. 2, No. 3, 2007, Publisher's website: www.inderscience.com, ISSN (Print) 1748-5711, ISSN (Online) 1748-572X, pp.: 451-477 **13** Astakhov, V. P.: **Metal Cutting Mechanics**, Boca Raton, FL, USA: CRC Press. 1999 **14** Johnson, G., Cook, W.: **A constitutive model and data for metals subjected to large strains, high strain rates and high temperatures**, 7th International Symposium on Ballistics, 1983, pp.: 541-547 **15** Jaspers, S.P.F.C., Dautzenberg, J.H.: **Material behavior in conditions similar to metal cutting: flow stress in the primary shear zone**, Journal of Materials Processing Technology, Vol. 122, 2002, pp.322-330. **16** Dirikolu, M.H., Childs, T.H.C., Maekawa, K.: Finite element simulation of chip flow in metal machining, International Journal of Mechanical Sciences, Vol. 43, 2001, pp.2699-2713. **17** Özel, T., Altan, M. T.: **Determination of workpiece flow stress and friction at thechip-tool contact for high-speed cutting**, International Journal of Machine Tools & Manufacture 40, 2000, pp.: 133-152. **18** Sartkulvanich, P., Altan, T., Göcmen, A.: **Effects of Flow stress and Friction Models in Finite Element Simulation of Orthogonal Cutting – a Sensitivity Analysis**, Machine Science and Technology, (2005) 9, pp.: 1-26. **19** Čep, R., Neslušan, M.; Barišič, B.: **Chip Formation Analysis during Hard Turning**. Strojarstvo, 2008, vol 50, No. 6, pp.: 337 – 345, ISSN 0562 – 1887. **20** Lee, E., Shaffer, B.: **The theory of plasticity applied to a problem of machining**, Journal of Applied Mechanics, Vol.: 73, 1951, p. 404-413. **21** Iwata, K., Osakada, K., Terasaka, Y.: **Process modeling of orthogonal cutting by the rigid-plastic finite element method**, ASME Journal of Engineering for Industry 106, 1984, pp.: 132-138. **22** Özel, T., Altan, M. T.: **Determination of workpiece flow stress and friction at thechip-tool contact for high-speed cutting**, International Journal of Machine Tools & Manufacture 40, 2000, pp.: 133-152. **23** Shaw, M. C.: **Metal Cutting Principles**, Oxford University Press, Oxford, 1984. **24** Ambati, R.: **Simulation and Analysis of Orthogonal Cutting and Drilling Processes using LS-DYNA**, Master of Science Thesis at University of Stuttgart, University of Stuttgart, Germany, December 2007-June 2008, p.: 71 **5** Nyiro, J.: **Results of analysis of cutting**, FMTU, Cluj Napoca, Romania, March 22-23, 2002, pp.: 109-112

Поступила в редколлегию 15.04.2011